Investigation of an 11mm diameter Twin Screw Granulator: Screw Element Performance and In-line Monitoring via Image Analysis

Ridade Sayin[1,2], Laura Martinez-Marcos[3,4], Juan G. Osorio[1,2], Paul Cruise[5], Ian Jones[5], Gavin W. Halbert[3,4], Dimitrios A. Lamprou[3,4*], James D. Litster[1,2,6*]**

[1]Center for Particulate Processes and Products, Purdue University, West Lafayette, Indiana, USA

[2]School of Chemical Engineering, Purdue University, West Lafayette, Indiana, USA

[3]Strathclyde Institute of Pharmacy and Biomedical Sciences (SIPBS), University of Strathclyde, Glasgow, UK

[4] EPSRC Centre for Innovative Manufacturing in Continuous Manufacturing and Crystallisation (CMAC), Technology and Innovation Centre, Glasgow, UK

[5]Innopharma Laboratories, Dublin, Ireland

[6]Industrial and Physical Pharmacy, Purdue University, West Lafayette, Indiana, USA

*Corresponding authors. Email address: jlitster@purdue.edu and dimitrios.lamprou@strath.ac.uk

Tel.: +1 765 496-2836, Fax: +1 765 494-0805

** Funded by Cancer Research UK

ABSTRACT

As twin screw granulation (TSG) provides one with many screw element options, characterization of each screw element is crucial in optimizing the screw configuration in order to obtain desired granule attributes. In this study, the performance of two different screw elements - distributive feed screws and kneading elements - was studied in an 11mm TSG at different liquid-to-solid (L/S) ratios. The kneading element configuration was found to break large granules more efficiently, leading to narrower granule size distributions. While pharmaceutical industry shifts towards continuous manufacturing, inline monitoring and process control are gaining importance. Granules from an 11mm TSG were analysed using the Eyecon^{TM}, a real-time high speed direct imaging system, which has been used to capture accurate particle size distribution and particle count. The size parameters and particle count were then assessed in terms of their ability to be a suitable control measure using the Shewhart control charts. d_{10} and particle count were found to be good indicators of the change in L/S ratio. However, d_{50} and d_{90} did not reflect the change, due to their inherent variability even when the process is at steady state.

Keywords: Twin Screw Granulation, In-line Image Analysis, Shewhart Control Charts, Continuous Pharmaceutical Manufacturing, Process Analytical Technology

1. Introduction

Nowadays, there is an imminent necessity for the pharmaceutical industry to deliver pharmaceutical products that comply with the highest quality standards. Regulatory authorities such as the US Food and Drug Administration (FDA) agency and the European Medicines Agency (EMA) are focusing their efforts towards the implementation of the new ICH Q10 “Pharmaceutical Quality System” guidelines that enable industrial manufacturers to put in place better controlled development and manufacturing practices (ICH Q10, 2008). One of the current challenges requires that pharmaceutical industries fully understand the relation between the manufacturing processing parameters or process performance and the critical quality attributes (CQA) of the final product. Therefore, the introduction of process analytical technologies (PAT) for continuous in-line monitoring of manufacturing processes is crucial to assure product quality throughout all the manufacturing stages. In this context, the interest towards the development of continuous manufacturing platforms for the production of pharmaceuticals has increasingly emerged.

One of the main areas that can be applied within a continuous manufacturing environment comprises the initial stages of development and production of pharmaceuticals, where twin-screw granulation (TSG) is being applied as an alternative to traditional batch manufacturing processes. TSG provides flexibility during manufacturing of commercial products as well as time and economic cost reduction that are currently important issues in the pharmaceutical arena. Moreover, the capability offered by TSG processes where it is possible to optimise the processing parameters to achieve high quality attributes of the end product is still being studied and this is where the application of in-line characterisation techniques plays a key role. Recently, Seem et al. (2015) reviewed literature related to twin screw granulation, where they emphasized the need for further process understanding and optimization. Screw element configuration is of crucial importance in determining the resulting granule attributes from a twin screw granulator (Djuric and Kleinebudde, 2008; Thompson and Sun, 2010) and its effects on resulting granule properties were extensively studied in literature using conveying elements (CE) (Thompson and Sun, 2010; Dhenge et al., 2012), kneading elements (KE) (Thompson and Sun, 2010; Mu and Thompson, 2012; El Hagrasy and Litster, 2013; Lee et al., 2012; Melkebeke et al., 2008;

Vercruysse et al., 2012, 2014, 2015; Kumar et al., 2014), distributive mixing elements (DME) (Thompson and Sun, 2010; Sayin et al., 2015; Vercruysse et al., 2015), distributive feed screw (DFS) (Vercruysse et al., 2015), and cutters (Vercruysse et al., 2015). The first attempt to elucidate the effect of screw configuration on granule and tablet properties was made by Djuric and Kleinebudde (2008), using a Leistritz Micro 27GL/28D. In their study, Djuric and Kleinebudde (2008) studied CE, KE, and DFS under the name of combing mixer elements. DFS was found to produce higher yield (granules in the range: 125 μm – 1250 μm) when compared to the same pitch CE, as well as less lumps (granules larger than 1250 μm). KE configurations with 30° reverse and 90° (neutral) advance angles gave the least porous granules among the screw configurations studied. Thompson and Sun (2010) studied distributive mixing elements (DME) in addition to CEs and the kneading blocks using an American Leistritz (Model ZSE-27 HP) twin screw extruder with no die. They suggest that intermeshing region of KEs is the key region in granule formation and the advance angle is of minor importance. Shah (2005) used 34 and 50mm twin screw extruders with no die to study CE, KE, and DFS under the name of chopper element. Further studies on the effect of screw configuration include use of a 16 mm Thermo Fisher twin-screw granulator to produce and characterise granule attributes by the inclusion of different screw elements such as conveying elements, kneading elements and distributive mixing elements (El Hagrasy and Litster, 2013; Sayin et al., 2015). Recently, an 11mm TSG has become available, and there are advantages for early stages of new product development due to the smaller amount of formulation that is required compared to 16 or 24mm TSGs. However, there are no reported studies on the use of the 11mm TSG and its performance as a granulator has not been assessed. In particular, the 11mm TSG offers a new screw element design, the distributive feed screw, whose performance has not been evaluated using a Thermo Fisher twin screw granulator.

Various PAT techniques for in-line measurement of continuous wet granulation processes have recently been studied. Soppela et al. (2011) compared the application of a 3D-imaging technique (FS3D) and a spatial filtering technique (SFT or also called Parsum) identifying good correlation values in the characterisation of granule particle size distribution and flowability properties. Further investigations regarding solid state transformations during continuous twin-screw wet granulation have been studied using Raman and Near-infrared (NIR) spectroscopy (Fonteyne et al., 2013). Moreover, Kumar et al., (2014) applied a near infrared chemical imaging system within residence time distribution (RTD) studies in a continuous TSG process, showing that variations in screw speed, material throughput, screw configuration, number and geometry of kneading elements have an impact on granule RTD and axial mixing degree achieved. Similar RTD studies on a TSG were performed by Lee et al., (2012) applying Positron Emission Particle Tracking (PEPT) technique where barrel design modifications were required. Moreover, previous granule characterisation studies performed by El Hagrasy and Litster (2013) showed a relation between the granulation rate processes involved in granule growth such as breakage or layering with granule shape by applying different screw configurations, kneading element advance angles and angle direction. Introduction of a high-speed imaging camera, such as the Eyecon^{TM} particle characteriser was reported (El Hagrasy et al., 2013) as a successful non-contact technique for in-line characterisation of TSG processes. Assessment of granule particle size distribution as well as granule shape enabled evaluation of granule growth based on parameter changes with variations in liquid to solid (L/S) ratios (El Hagrasy et al., 2013).

This study aims at characterizing the distributive feed screw and assessing capability of a high-speed imaging technique for the in-line control of granule size parameters produced by an 11mm TSG. Particle attributes such as particle size and liquid distributions are presented from offline analyses. The measurement of particle attributes using an in-line method provides a better understanding of real-time product characteristics providing a design of space network for continuous manufacturing applications. The TSG process comprising a distributive feed screw (DFS) as main granulation element is introduced and characterised in a Thermo Fisher twin screw granulator for the first time. In-line characterisation of granule size parameters are obtained using a high-speed imaging camera attached to a Thermo Scientific® Process 11 twin-screw granulator. Offline particle size and liquid distributions obtained using DFS are also compared to values achieved using a kneading element (KE) configuration comprised of 7 kneading elements with 90-degree advance angle. Further analytical procedures included data processing and elaboration of Shewhart control charts to evaluate the applicability of particle size parameters such as d_{10}, d_{50}, d_{90} and particle count to monitor the influence of small process variations in L/S ratio values.

2. Materials and Methods

2.1 Granulation Experiments

In this study, a placebo formulation composed of α-lactose monohydrate (Pharmatose 200M, 73.5%), microcrystalline cellulose (Avicel PH101, 20%), hydroxypropylmethyl cellulose (Hypromellose, 5%) and croscarmellose sodium (Ac-Di-Sol, 1.5%) was used. These dry ingredients were pre-mixed using a Turbula® T2F mixer (Glen Mills Inc., New Jersey, United

States) in batches of 500 g of blend for 20 min. A volumetric feeder (DDSR20, Brabender Technologie GmbH, Duisburg, Germany) was used to feed the blend into the 11mm TSG (Process 11, 40:1 L/D, Thermo Fisher Scientific, Karlsruhe, Germany) operating at 482 rpm. The powder feed rate was adjusted to 1.11 kg h^{-1}. A 0.1% (w/w) aqueous solution of nigrosin black dye (Sigma Aldrich Corp., St. Louis, MO) was used as the granulation liquid. The liquid was fed into the TSG using a peristaltic pump (Thermo Fisher Scientific, Karlsruhe, Germany) at different rates to achieve liquid to solid (L/S) ratios of 0.15, 0.20, 0.25, and 0.30.

Two screw configurations were used. Distributive feed screw (DFS) and kneading elements (KE) were the screws of interest in these configurations, as DFS is expected to improve GSD when compared to conveying elements and KEs were found to break lumps without causing shear elongation by El Hagrasy and Litster (2013). In both cases, four 1-D conveying elements were placed in the downstream of screws of interest. Conveying elements were used in the upstream of the screws of interest to convey the mixture towards these screw elements. A schematic of the screw configurations is provided in Figure 1.

Figure 1 shows the liquid and powder feed zones, which are the second and third zones of the granulator, respectively. SoI refers to screw element of interest. In the first screw design, one pair of DFS was used as the screw of interest. In the second design, SoI was a kneading block consisting of 7 kneading elements with 90-degree advance angle. In a recent study, El Hagrasy and Litster (2013) showed that using seven KEs instead of three or five improves the liquid distribution. Pictures of DFS and KEs are provided in Figure 2.

2.2 Offline Granule Size Analysis

The granules collected from each experiment were spread on a tray and dried at room temperature for 48 hours. They were then split using a Laborette 27 rotary cone sample divider (Fritsch GmbH, Idar-Oberstein, Germany) to obtain representative samples. Granule size distribution was measured via sieve analysis using a √2 series of sieves from 63 µm to 8 mm. The normalized mass frequency with respect to the logarithm of particle size was plotted according to equation 1 (Allen, 2003):

$$f_i(lnx) = \frac{y_i}{\ln(^{x_i}/_{x_{i-1}})} \qquad \text{Eq. 1}$$

where, y_i is the mass fraction in size interval i and x_i is the upper limit of the size interval i.

2.3 Liquid Distribution

The liquid distribution (LD) method used is similar to the one reported by Smirani-Khayati et al. (2009) and has been presented in El Hagrasy and Litster (2013) in detail. Briefly, after completing the sieve analysis, three granule samples from each sieve fraction were dissolved in water separately and sonicated for 1 h. The sonicated samples were further diluted and centrifuged. The supernatant nigrosin dye concentration was measured using a UV/Vis spectrophotometer (Cary UV Vis 300, Agilent, Wilmington, DE) at $\lambda_{max} = 574\ nm$.

2.4 Granule Porosity

A helium pycnometer (AccuPyc, Micromeritics) was used to measure the true density of the granules. The granule envelope density measurement was then performed using an envelope density pycnometer (Geopyc, Micromeritics). Granules in the size fraction 1.0–1.4 mm were used for the measurements. The following equation was then used to calculate granule porosity ($\varepsilon_{granules}$).

$$\varepsilon_{granules} = 1 - \frac{\rho_g}{\rho_s} \quad \text{Eq. 2}$$

where ρ_g and ρ_s are the envelope and true density of the granules, respectively.

2.5 Granulation Experiments for image analysis

For the image analysis using the DFS configuration, a screw speed of 724 rpm and a powder feed rate of 3.9 kg h^{-1} were used. A screw speed of 482 rpm was used for the 7KE90 configuration with a powder feed rate of 0.66 kg h^{-1}. In both cases, the experiments were run at four L/S ratios namely, 0.15, 0.20, 0.25, and 0.30. The same powder blend and granulation liquid were used as in the case of granulation experiments, for both screw configurations. Temperature was not controlled during the experiments since temperature control requires the die to be assembled to the TSG. This is because the TSG used was originally built as an extruder and was modified to be used as a granulator. When performing experiments using the 7KE90 configuration, the metal chute was heated via a thin metal coil attached to it from outside, which prevented the un-granulated powder sticking onto the chute.

2.6 In-line Image Analysis & Experimental Setup

The Eyecon™ Particle Characterizer was used for the in-line granule size analysis. Granule images were recorded while running the TSG and collecting the granule samples. Figure 3 shows the experimental setup with the integrated TSG-camera system.

The metal chute presented by El Hagrasy et al. (2013) was attached to the exit of the TSG in order to provide a representative sample to the camera. With its narrowing design, the chute directs the granules into the focus of the camera. Its inclination allows the granules to flow freely, allowing random orientation of the granules to be captured. El Hagrasy et al. (2013) has described the working principles of Eyecon™ camera in detail. In brief, the camera emits red-green-blue (RGB) light onto the sample, creating 3D images of the particles. It can detect particles between 50 and 3000 microns flowing with a speed up to 10 m s^{-1}. It collects size (e.g. d_{10}, d_{50}, d_{90}) and shape (e.g. average aspect ratio) information in two seconds per image and uses a 30 sec moving window to calculate the average parameter values. In this study, the camera measures the size of wet granules immediately after they exit the granulator, being a non-destructive method. It measures the minimum and maximum diameters of a particle, by fitting an ellipse. The software then takes the average of these two diameters and calculates the volume of the particle assuming that it is a sphere of this average diameter. It assumes that all the particles have the same density and calculates the size parameters. Due to the RGB light, it can detect the boundaries of each particle and differentiate the ones that are overlapping or partially in the area of view. Those particles can then be excluded from the calculations, resulting in the values obtained using only the particles that are completely within the field of view.

3. Results and Discussion

3.1 DFS characterization and comparison to 7KE90 screw configuration

Granule size distributions obtained via sieve analysis at four different L/S ratios using the DFS and KE configurations are presented in Figure 4.

In Figure 4a, the granule size distributions obtained using the two configurations are both bimodal. Bimodality of the 7KE90 configuration has been reported previously by El Hagrasy and Litster (2013) using a 16mm TSG. Additionally, both size distributions have similar spans, the one from the DFS configuration being a little larger. As the L/S ratio increases, the amount of coarse granules (larger than 1 mm) increase and the amount of un-granulated fines decrease since there is more liquid to form nuclei and for powder layering. In Figures 4b and 4c the two configurations give similar size distributions with 7KE90 configuration having more breakage of the coarse granules. In Figure 4d, the difference between the GSDs increased due to DFS configuration having more large granules. This shows that the kneading element configuration breaks the large granules more efficiently, resulting in a narrower size distribution. The DFS configuration is not as good in breaking the large granules that are formed at high L/S ratios.

Figure 5 presents the amounts of fines (granules smaller than 125 μm) and coarse granules (larger than 1 mm) as a function of L/S for both configurations. This analysis is important since both fines and coarse granules are undesirable in the downstream processes.

In Figure 5a, the fraction of fines decreases with increasing L/S ratio for both screw configurations, with the decrease in DFS being a little steeper. In Figure 5c, the increase in L/S ratio brings the increase in the coarse granules for both configurations. The fraction of coarse granules in 7KE90 configuration is less than that of DFS at all L/S values, indicating a better breakage process in the case of 7KE90. In Figure 5b, 7KE90 configuration produces a higher fraction of granules that are in the range between 125 μm and 1 mm, due to its lower fraction of coarse granules. The fraction of granules in the desired range goes through a maximum at the

L/S ratio of 0.25. To better understand mixing and breakage behaviour, liquid distribution analysis was performed. Figure 6 presents the analysis results for both screw configurations.

Figure 6 shows that 7KE90 configuration distributes the liquid better than the DFS configuration due to more efficient breakage of large granules, indicated by the more horizontal curve. In case of the 7KE90 configuration, large granules have a liquid content that is close to the liquid to solid ratio, suggesting that layering is taking place. This is in accordance with El Hagrasy and Lister's (2013) findings, where they elucidated granulation rate processes taking place in the kneading section of TSG. In case of the DFS configuration however, liquid content is a strong function of granule size, where large granules have more liquid per mass than smaller granules. Liquid distribution is an important factor, whether the binder is introduced in liquid or powder form, in obtaining granules with similar attributes such as strength.

Granule porosity results are provided in Figure 7.

The 7KE90 configuration results in granules that are less porous than the DFS configuration, indicating more consolidation taking place in 7KE90. This is in accordance with the study of Djuric and Kleinebudde (2008), where two different lengths of KEs with 90° advance angle were used as well as two different pitches of DFS of different length. In Figure 7, there's a decreasing trend in porosity with increasing L/S ratio for both screw configurations except for DFS at the highest L/S ratio, where a slight increase is observed. The two screw configurations differ also in terms of practicality. The minimum and maximum torque values recorded during the experiments are provided in Table 1, as well as maximum temperatures observed.

In Table 1, the maximum torque values are the highest values that were observed during the experiments. In most of the cases, the torque values fluctuated and were not stationary at the maximum level for more than a few seconds. The 7KE90 configuration results in much higher temperatures and torque values when compared to DFS, accompanied by a loud noise. These maximum temperature and torque values were observed to drop significantly when a much lower powder feed rate was used, keeping all other parameters the same. These agree with the findings of Shah (2005), where surging was observed when KEs with 90° advance angle were used, which was reduced with the use of DFS (mentioned as chopper element in their study), after the removal of KEs.

Caution needs to be exercised in comparing these results for DFS and KE configurations in the 11mm TSG with experimental data from 16mm TSG in the literature. We do expect the breakage rates of granules to vary with the change in geometry as the diameter of the TSG is increased. Thus direct comparison of granule size distributions is not advised until scaling rules have been developed and validated.

3.2 In-line size monitoring of the granules via Eyecon^TM^ camera

Eyecon™ camera software outputs a CSV. file containing granule size parameter measurements (e.g. d_{10}, d_{50}) from each image with 2-3 sec. intervals. Figure 8 shows the granule size parameter results from the DFS configuration at four L/S ratios. This figure was constructed by combining a one-minute section from each experimental data set at different L/S ratios.

In Figure 8, the granule size parameter and particle count values are similar for the first three L/S ratios. This can partly be attributed to inherent variance in data that may prevent observation of a slight increase. At the highest L/S ratio, there's an increase in the granule size parameters and decrease in count. At the L/S of 0.15, the number of particles captured by Eyecon™ in each image is around 200. This low number can be attributed to relatively small window of the imaging technique used, where it can be increased by improving sample presentation. Here, relatively small window of operation is in the direction perpendicular to the lens plane. As the flowing granules cover a three-dimensional space, camera focus adjustment becomes of key importance in capturing a representative sample of those granules. The fluctuation in size parameters can be attributed to fluctuations inherent in the process, originating from the powder and liquid feeding methods. The variation in the data increase as one goes from particle count and d_{10} to d_{50} and d_{90}, which is in accordance with El Hagrasy et al. (2013) work.

3.3 Shewhart control charts for the Eyecon™ data for size parameters (d_{10}, d_{50}, d_{90} and particle count)

In-line process control has become of key importance for continuous processes. In the case of continuous granulation, granule size is a crucial attribute to be maintained due to its effect on downstream material properties such as tabletability. El Hagrasy et al. (2013) studied sensitivity of Eyecon™ camera using five kneading elements with an advance angle of 60° in the forward direction (clockwise) in a 16mm TSG, where they made use of the Shewhart control charts (Oakland, 2003) to see the appropriate measures to be used for control purposes. The same technique was used in this study to assess the ability of different measures to reflect the changes in L/S ratio. As the use of control charts requires absence of autocorrelation in the data points in time series, the Durbin-Watson statistic was used to test the autocorrelation in the data from each experiment. Durbin-Watson statistic values were found to be higher than the corresponding upper significance limits at five percent level of significance, indicating that no autocorrelation exists in the data. To construct the control charts, the centerline (CL), upper control limit (UCL), and lower control limit (LCL) were calculated using equations 3 – 5:

$$CL = \mu \qquad \text{Eq. 3}$$

$$UCL = \mu + 3\frac{\sigma}{\sqrt{n}} \qquad \text{Eq. 4}$$

$$LCL = \mu - 3\frac{\sigma}{\sqrt{n}} \qquad \text{Eq. 5}$$

where, μ and σ are the estimated mean and standard deviation and n is the sample size, which was taken as five.

When control charts are used, variability of the data under control is measured and the control limits beyond which the system will be treated to be out of control are determined to be a factor times this variability above and below the centerline. To obtain the sensitivity of Eyecon™ measurements to changes in L/S ratio, a four-minute section is taken from experiments with different L/S ratios and plotted in succession. The mean control charts for size parameters and particle count using DFS and 7KE90 configurations are provided in Figures 9 and 10, respectively. In Figure 9, the control limits were set using the data at the L/S ratio of 0.30 and compared against that at 0.20. In Figure 10 however, the limits were set at the L/S ratio of 0.15 and tested using another experiment at 0.25 L/S ratio.

In Figures 9a and 9b, d_{50} and d_{90} have such high inherent variation when the system is at steady state that most of the time those parameters seem to be under control even after the L/S ratio has changed. This makes the two size parameters not suitable as control measures. This agrees with the results obtained by El Hagrasy et al. (2013), where a 16mm TSG was used with a configuration consisting of CEs and 5 KEs with 60° advance angle in the forward direction. In Figure 10a, d_{50} reflects the increase in L/S ratio. However, most of the d_{90} values are within the control limits even after the L/S is changed. On the other hand, as d_{10} and particle count have relatively less variation when compared to d_{50} and d_{90}, they are more sensitive to changes in L/S in case of both screw configurations and fall out of the control limits most of the time when L/S ratio is changed. Figure 11 shows representative images captured via Eyecon™ camera during experiments using 7KE90 configuration at three L/S values.

Figure 11a corresponds to the results in Figure 10, using a L/S ratio of 0.15 and Figure 11b corresponds to those using a L/S ratio of 0.25. Figure 11 shows that larger granules are obtained at higher L/S ratios. Also, as the L/S ratio increases, amount of fines decrease, as well as total number of granules, where these results are in accordance with El Hagrasy et al. work (2013).

4. Conclusions

Distributive feed screw may improve the size distribution when compared to regular conveying elements. However, the DFS configuration is not as efficient in breaking the large granules when compared to 7KE90 configuration, as shown by granule size and liquid distributions. Nevertheless, 7KE90 configuration causes an increase in the temperature and torque, accompanied with a loud noise at relatively high powder feed rates. This was not observed while running the experiments with the DFS configuration. It indicates that DFS will be able to give a broader design space than the 7KE90 configuration. In terms of the use of in-line imaging for control of TSG, Eyecon™ camera was able to detect the increase in size and decrease in count when the L/S ratio was changed. Four parameters were investigated for their potential use in process control with Eyecon™ camera. d50 and d90 were measured at different L/S ratios and found not to be good measures for control purposes due to their inherent variability. On the other hand, d10 and particle count were sensitive to changes in L/S ratio and shown to be good measures for process control, in an 11mm TSG. Once the inherent variation in the granule properties at steady state are known, Eyecon™ camera can be used as a part of the control mechanism.

Acknowledgements

The authors would like to thank EPSRC and the Doctoral Training Centre in Continuous Manufacturing and Crystallisation for funding part of this work.

References

Allen, T., 2003. Powder Sampling and Particle Size Determination, first ed. Elsevier, Amsterdam.

Dhenge, R.M., Washino, K., Cartwright, J.J., Hounslow, M.J., Salman, A.D., 2013. Twin screw granulation using conveying screws: Effects of viscosity of granulation liquids and flow of powders. Powder Technol. 238, 77-90.

Djuric, D., Kleinebudde, P., 2008. Impact of Screw Elements on Continuous Granulation with a Twin Screw Extruder. J. Pharm. Sci. 97, 4934-4942.

El Hagrasy, A.S., Cruise, P., Jones, I., Litster, J.D., 2013. In-line Size Monitoring of a Twin Screw Granulation Process Using High-Speed Imaging. J. Pharm. Innov. 8, 90-98.

El Hagrasy, A.S., Litster, J.D., 2013. Granulation rate processes in the kneading elements of a twin screw granulator. AIChE J. 59, 4100-4115.

Guideline, I.H.T., 2008. Pharmaceutical quality system q10. Current Step 4.

Fonteyne, M., Vercruysse, J., Diaz, D.C., Gildemyn, D., Vervaet, C., Remon, J.P., De Beer, T., 2013. Real-time assessment of critical quality attributes of a continuous granulation process. Pharm. Dev. Technol. 18, 85-97.

Kumar, A., Vercruysse, J., Toiviainen, M., Panouillot, P.E., Juuti, M., Vanhoorne, V., Vervaet, C., Remon, J.P., Gernaey, K.V., De Beer, T., Nopens, I., 2014. Mixing and transport during pharmaceutical twin-screw wet granulation: experimental analysis via chemical imaging. Eur. J. Pharm. Biopharm. 87(2), 279-289.

Lee, K.T., Ingram, A., Rowson, N.A., 2012. Twin screw wet granulation: the study of a continuous twin screw granulator using Positron Emission Particle Tracking (PEPT) technique. Eur. J. Pharm. Biopharm. 81, 666-673.

Mu, B., Thompson, M.R. 2012. Examining the mechanics of granulation with a hot melt binder in a twin-screw extruder. Chem. Eng. Sci. 81, 46-56.

Oakland, J.S., 2003. Statistical Process Control, 5th ed. Butterworth-Heinemann, Burlington.

Sayin, R., El Hagrasy, A.S., Litster, J.D., 2015. Distributive mixing elements: Towards improved granules attributes from a twin screw granulation process. Chem. Eng. Sci. 125, 165-175.

Seem, T.C., Rowson, N.A., Ingram, A., Huang, Z., Yu, S., de Matas, M., Gabbott, I., Reynolds, G.K., 2015. Twin screw granulation—A literature review. Powder Technol. 276, 89-102.

Shah, U., 2005. Use of a Modified Twin Screw Extruder to Develop a High-Strength Tablet Dosage Form. Pharm. Technol. 29, 52-66.

Smirani-Khayati N., Falk V., Bardin-Monnier N., Marchal-Heussler L., 2009. Binder liquid distribution during granulation process and its relationship to granule size distribution. Powder Technol. 195(2), 105–112.

Soppela, I., Airaksinen, S., Hatara, J., Raikkonen, H., Antikainen, O., Yliruusi, J., Sandler, N., 2011. Rapid particle size measurement using 3D surface imaging. AAPS Pharm. Sci. Technol. 12, 476-484.

Thompson, M.R., Sun, J., 2009. Wet Granulation in a Twin-Screw Extruder: Implications of Screw Design. J. Pharm. Sci. 99, 2090-2103.

Van Melkebeke, B., Vervaet, C., Remon, J.P. 2008. Validation of a continuous granulation process using a twin-screw extruder. Int. J. Pharm. 356(1), 224-230.

Vercruysse, J., Cordoba Díaz, D., Peeters, E., Fonteyne, M., Delaet, U., Van Assche, I., De Beer, T., Remon, J.P., Vervaet, C., 2012. Continuous twin screw granulation: influence of process variables on granule and tablet quality. Eur. J. Pharm. Biopharm. 82(1), 205-211.

Vercruysse, J., Toiviainen, M., Fonteyne, M., Helkimo, N., Ketolainen, J., Juuti, M., Delaet, U., Van Assche, I., Remon, J.P., Vervaet, C., De Beer, T., 2014. Visualization and understanding of the granulation liquid mixing and distribution during continuous twin screw granulation using NIR chemical imaging. Eur. J. Pharm. Biopharm. 86(3), 383-392.

Vercruysse, J., Burggraeve, A., Fonteyne, M., Cappuyns, P., Delaet, U., Van Assche, I., De Beer, T., Remon, J.P., Vervaet, C., 2015. Impact of screw configuration on the particle size distribution of granules produced by twin screw granulation. Int. J. Pharm. 479(1), 171-180.

Figure captions

Figure 1: Schematic of the screw configurations used.

Figure 2: Picture of a) a DFS and b) KEs.

Figure 3: Experimental setup showing the 11mm TSG (A), Powder feeder (B), Peristaltic pump (C), Computer screen showing real time images from Eyecon^{TM} camera (D), Eyecon^{TM} camera (E), and the Metal chute presenting the sample (F).

Figure 4: GSDs from DFS and 7KE90 configurations at L/S ratio of 0.15 (a), 0.20 (b), 0.25 (c), and 0.30 (d).

Figure 5: Granule size parameters d10 (a), d50 (b), and d90 (c) as a function of L/S ratio for DFS and 7KE90 configurations.

Figure 6: Liquid distribution results for both screw configurations.

Figure 7: Per cent porosity of granules as a function of L/S ratio.

Figure 8: Granule size parameters (d10, d50, and d90) and particle count at different L/S ratios.

Figure 9: Shewhart control charts for the size parameters d10 (a), d50 (b), d90 (c), and particle count (d) using DFS configuration.

Figure 10: Shewhart control charts for the size parameters d10 (a), d50 (b), d90 (c), and particle count (d) using KE configuration.

Figure 11. Representative images captured during experiments using 7KE90 configuration at L/S ratio of 0.15 (a), 0.25 (b), 0.30 (c).

Table 1. Min. and max.Torque and max. temperature values observed during the experiments

	DFS			KE		
L/S Ratio	Min Torque (Nm)	Max Torque (Nm)	T (°C)	Min Torque (Nm)	Max Torque (Nm)	T (°C)
0.15	0.7	0.9	29	1	3	60
0.20	0.8	0.9	28	0.9	3.4	59
0.25	0.8	0.8	33	1.2	3.9	56
0.30	0.8	0.9	34	0.9	3	57

Description:

Table 1 shows the minimum and maximum torque values and maximum temperatures observed during the experiments using both screw configurations.

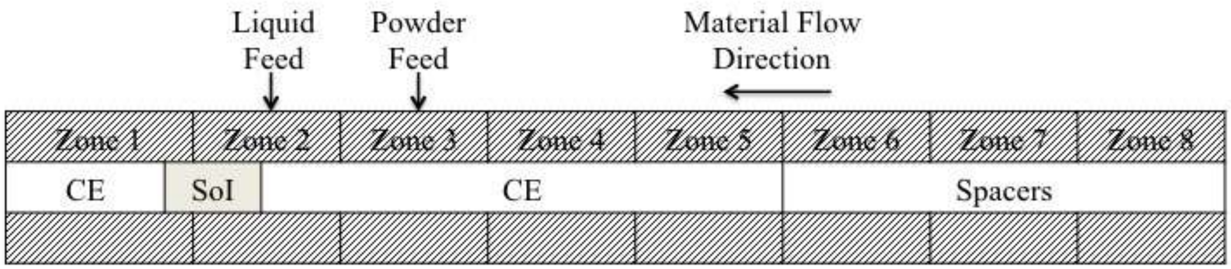
Liquid Feed
Powder Feed
Material Flow Direction
Zone 1
Zone 2
Zone 3
Zone 4
Zone 5
Zone 6
Zone 7
Zone 8
CE
SoI
CE
Spacers

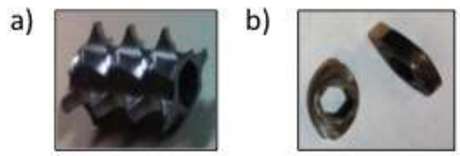
a)
b)

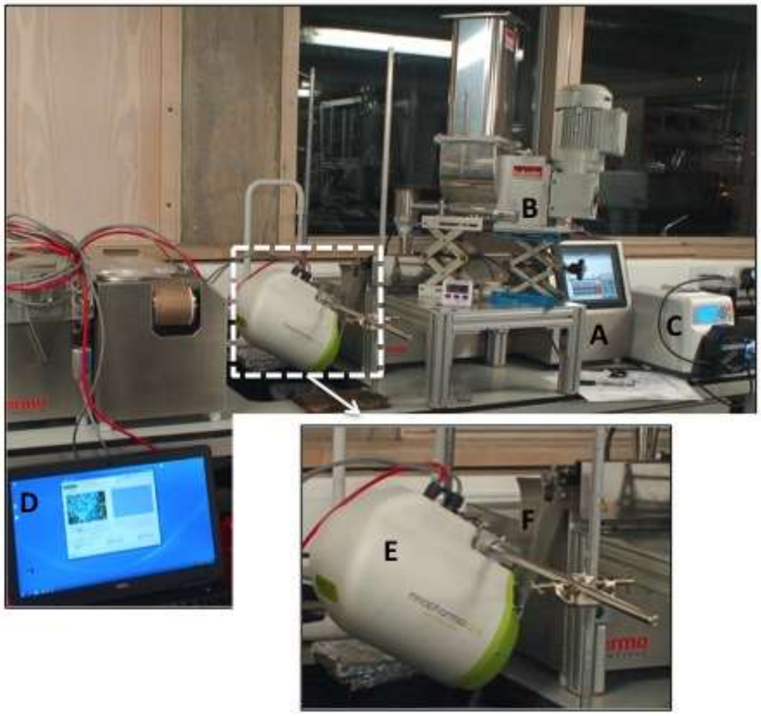
B
A
C
D
E
F

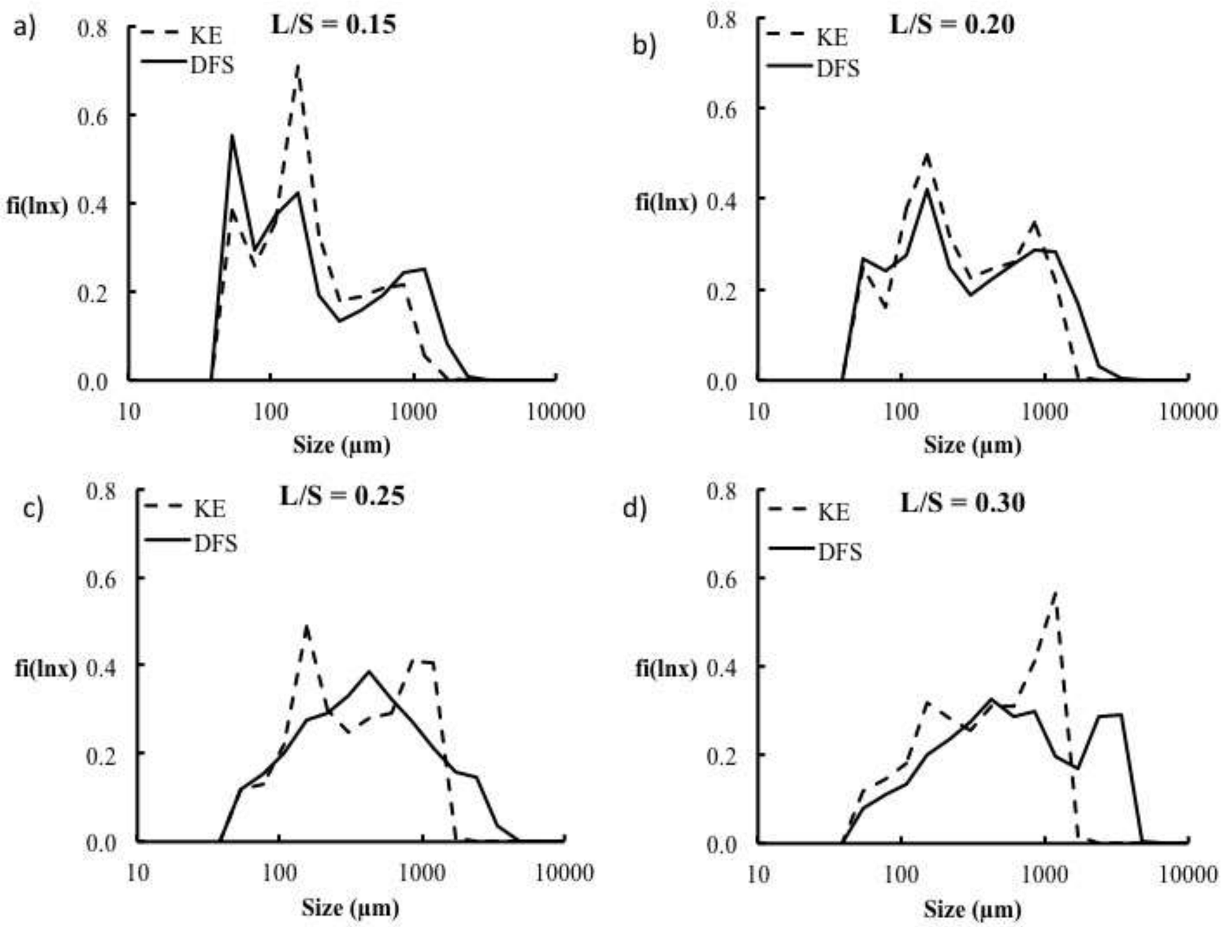
a)
L/S = 0.15
KE
DFS
fi(lnx)
0.0
0.2
0.4
0.6
0.8
10
100
1000
10000
Size (µm)
b)
L/S = 0.20
KE
DFS
fi(lnx)
Size (µm)
c)
L/S = 0.25
KE
DFS
fi(lnx)
Size (µm)
d)
L/S = 0.30
KE
DFS
fi(lnx)
Size (µm)

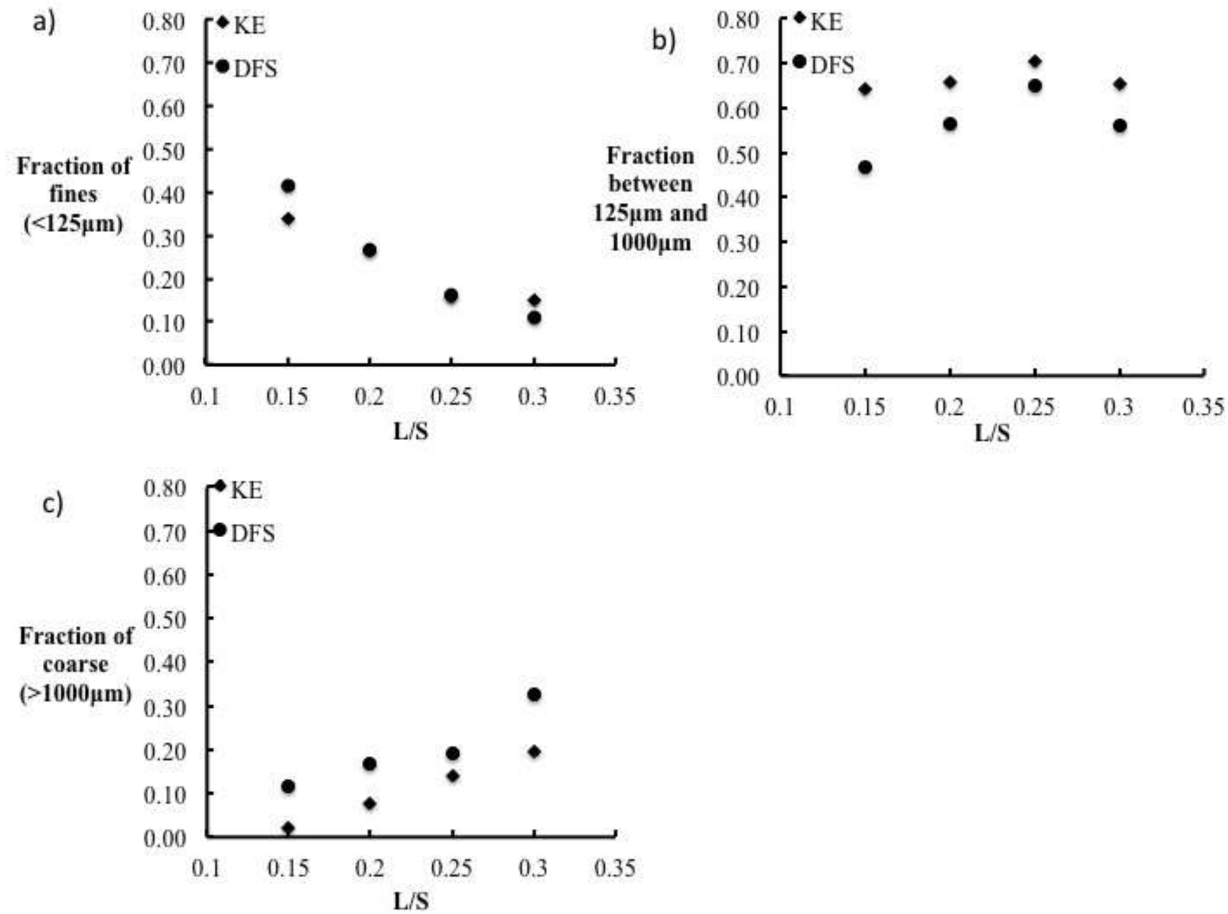
a)
KE
DFS
Fraction of fines (<125μm)
0.80
0.70
0.60
0.50
0.40
0.30
0.20
0.10
0.00
0.1
0.15
0.2
0.25
0.3
0.35
L/S
b)
KE
DFS
Fraction between 125μm and 1000μm
L/S
c)
KE
DFS
Fraction of coarse (>1000μm)
L/S

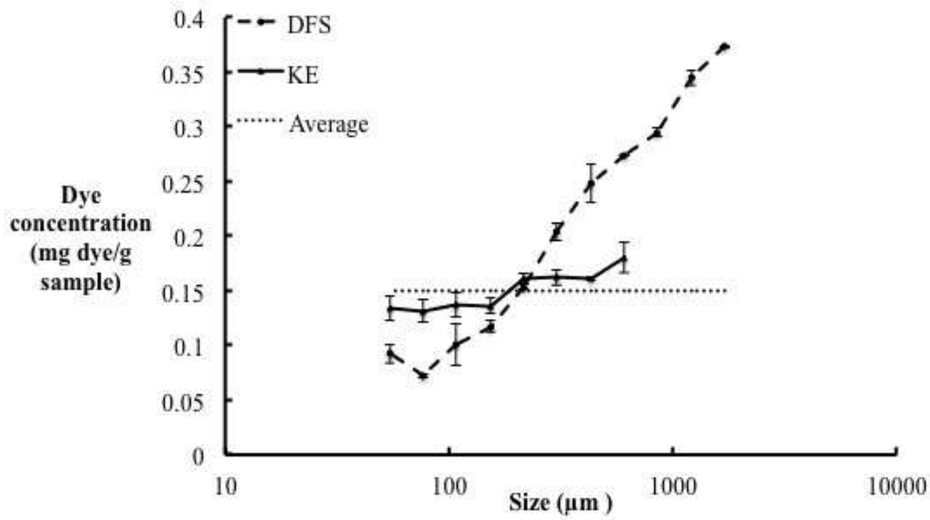
DFS
KE
Average
Dye concentration (mg dye/g sample)
0.4
0.35
0.3
0.25
0.2
0.15
0.1
0.05
0
10
100
1000
10000
Size (µm)

486

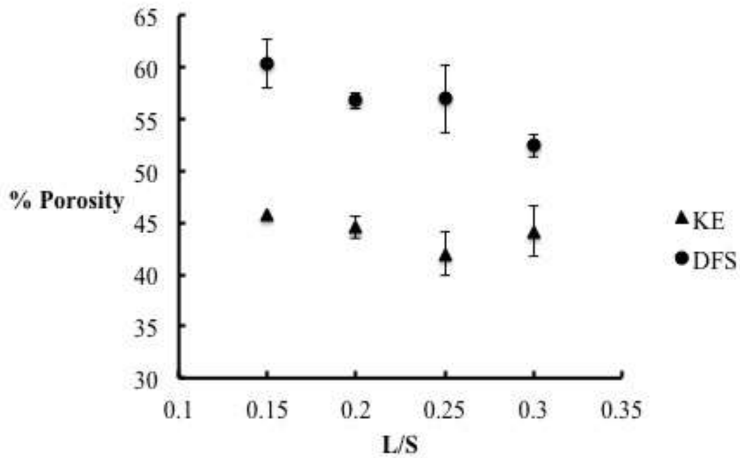

487

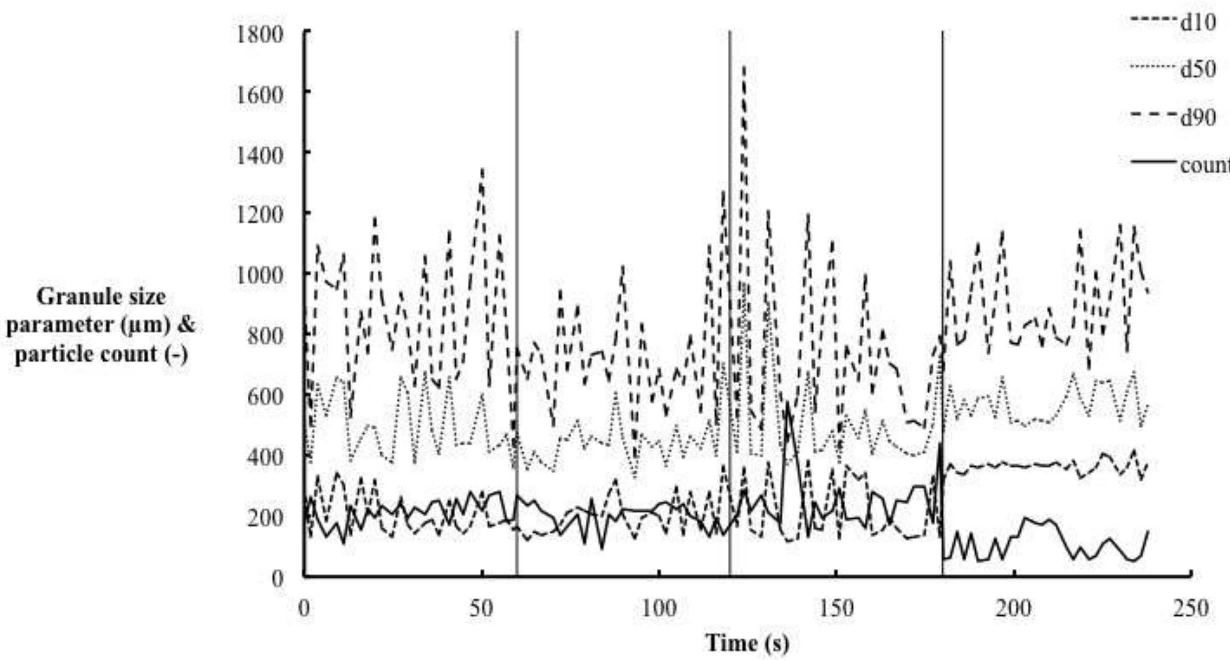
Granule size parameter (µm) & particle count (-)
1800
1600
1400
1200
1000
800
600
400
200
0
0
50
100
150
200
250
Time (s)
d10
d50
d90
count

488

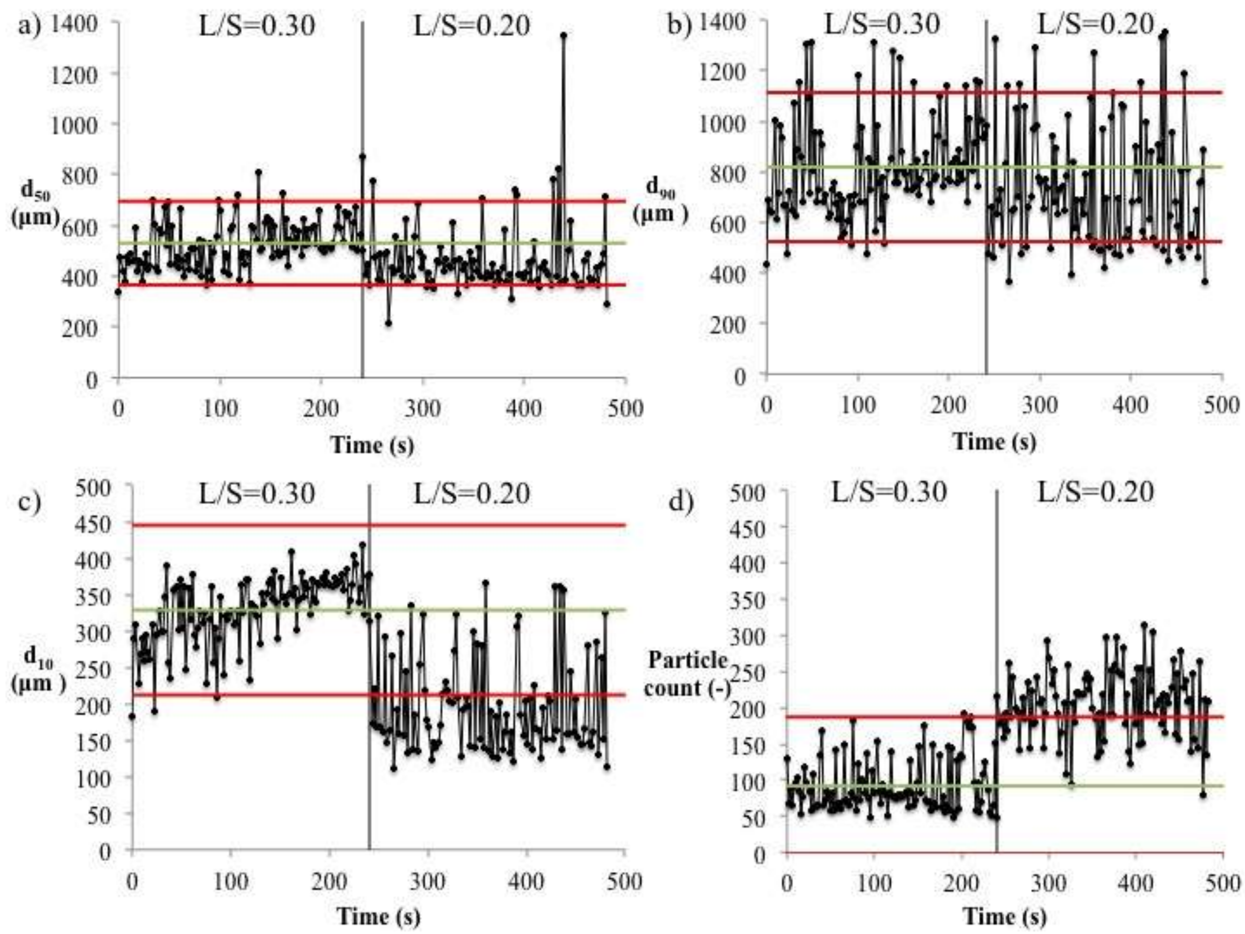
a)
L/S=0.30
L/S=0.20
d50 (µm)
Time (s)
b)
L/S=0.30
L/S=0.20
d90 (µm)
Time (s)
c)
L/S=0.30
L/S=0.20
d10 (µm)
Time (s)
d)
L/S=0.30
L/S=0.20
Particle count (-)
Time (s)

490

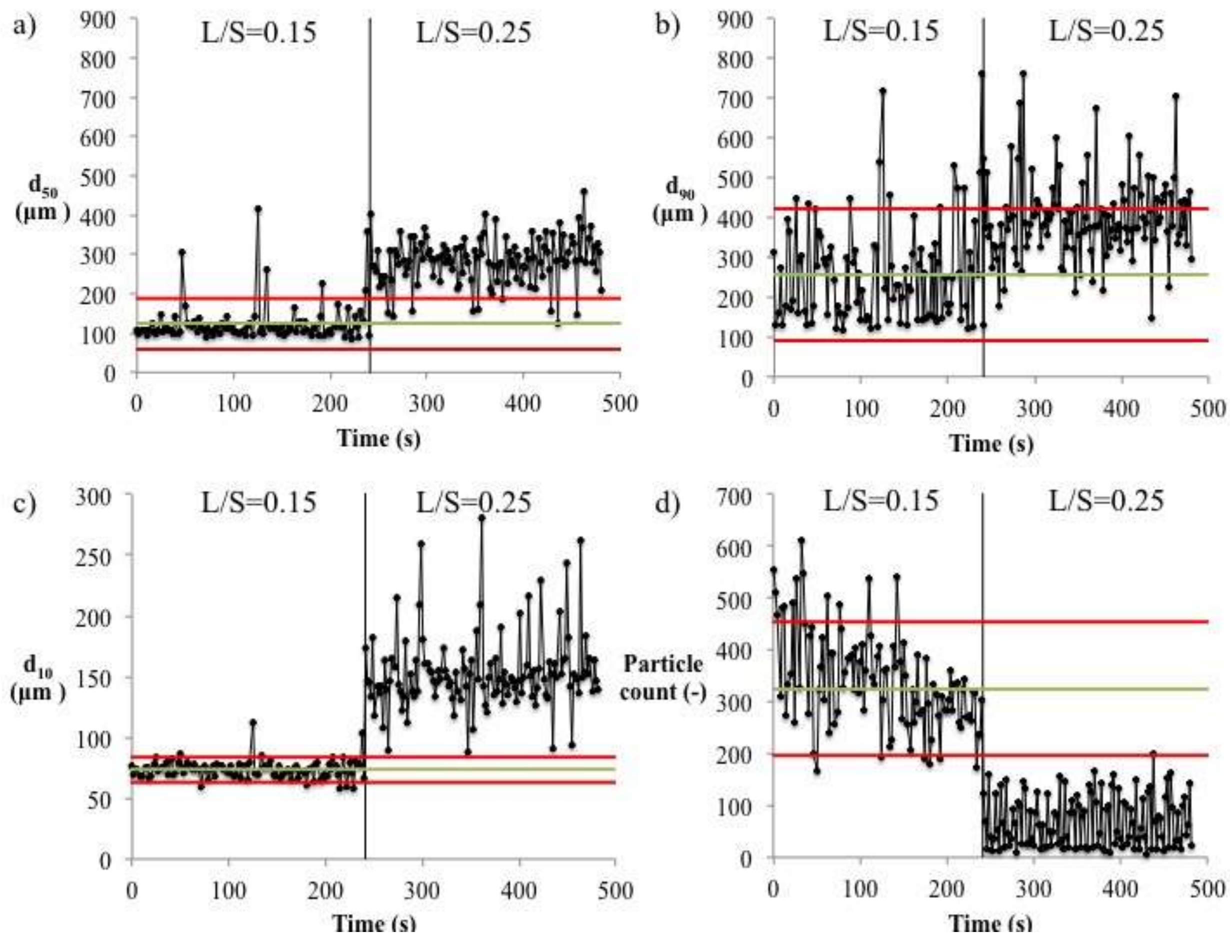
a)
L/S=0.15
L/S=0.25
d50 (µm)
Time (s)
b)
L/S=0.15
L/S=0.25
d90 (µm)
Time (s)
c)
L/S=0.15
L/S=0.25
d10 (µm)
Time (s)
d)
L/S=0.15
L/S=0.25
Particle count (-)
Time (s)

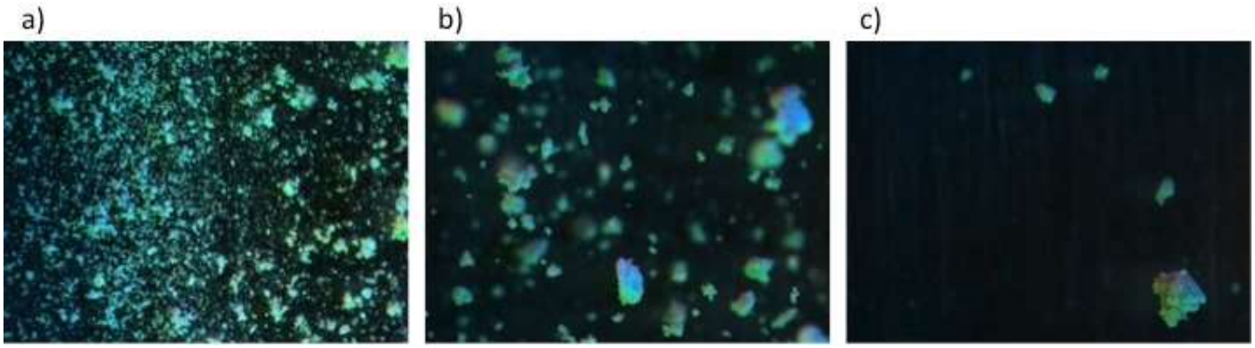
a)
b)
c)